Nanosecond time-scale Vlasov-Fokker-Planck laser-plasma simulation in a moving ion background

C. P. Ridgers and R. J. Kingham
Blackett Laboratory, Imperial College of Science, Technology and Medicine, London, SW7 2AZ, UK

Main contact email address christopher.ridgers@imperial.ac.uk

Introduction

Current interest in direct and indirect drive inertial confinement fusion (ICF) has emphasized the value of studying long-pulse laser-plasma interactions. Importantly such physics involves a significant departure from Braginskii transport theory[1]. We are currently interested in the development of the computational tools to study such a demanding theoretical situation; one which requires correct treatment of electron kinetics in the presence of a moving ion background. There is no kinetic code available today which can do this over the requisite nanosecond timescale including the effects of collisions and magnetic fields. In the regime of interest ion non-local effects are unimportant, thus one may treat them as a fluid. As a result we have developed a hybrid kinetic-hydrodynamic code. This treats the electrons kinetically using the code IMPACT[2] (Implicit Magnetized Plasma and Collisional Transport); we have coupled hydrodynamic ion motion to this. The resulting code allows nanosecond laser-plasma simulation in two spatial (three velocity) dimensions, including the effects of self-consistent magnetic fields and ion motion.

The Model

We solve the Vlasov-Fokker-Planck (VFP) equation for the electrons, i.e.:

$$\left[\frac{\partial}{\partial t}+\mathbf{v}\cdot\nabla_r-\frac{e}{m_e}(\mathbf{E}+\mathbf{v}\times\mathbf{B})\cdot\nabla_v\right]f(\mathbf{v},\mathbf{r},t)=$$
$$-\nabla_v\cdot\left[\frac{f(\mathbf{v},\mathbf{r},t)\langle\Delta\mathbf{v}\rangle}{\Delta t}\right]+\frac{1}{2}\nabla_v\nabla_v:\left[\frac{f(\mathbf{v},\mathbf{r},t)\langle\Delta\mathbf{v}\Delta\mathbf{v}\rangle}{\Delta t}\right] \quad (1)$$

The distribution function is represented by $f(\mathbf{v},\mathbf{r},t)$, the macroscopic electric and magnetic fields are given by **E** and **B** respectively. If we are to include ion motion in our model we need to transform equation (1) into the *average* rest frame of the ions – i.e. the frame moving at the local ion fluid velocity. We define this velocity as **C** – a function of position and time. We use **w** to represent the electron's velocity coordinate to distinguish it from **v**; they are related by $\mathbf{v}=\mathbf{w}+\mathbf{C}(\mathbf{r},t)$. Performing this transformation yields:

$$\frac{\partial f}{\partial t}+C_k\frac{\partial f}{\partial r_k}+w_k\frac{\partial f}{\partial r_k}+$$
$$\left\{a_k+\left[\mathbf{w}\times\omega\right]_k-\frac{\partial C_k}{\partial t}-w_j\frac{\partial C_k}{\partial r_j}-C_j\frac{\partial C_k}{\partial r_j}+\left[\mathbf{C}\times\omega\right]_k\right\}\frac{\partial f}{\partial w_k}=\left(\frac{\delta f}{\delta t}\right)_{coll} \quad (2)$$

In the above equation the electric and magnetic fields are normalized ($\mathbf{a}=-e\mathbf{E}/m_e$, $\omega=-e\mathbf{B}/m_e$). Further progress is made by expanding the distribution function in terms of the Cartesian tensors[3]:

$$f(\mathbf{w},\mathbf{r},t)=f_0(w,\mathbf{r},t)+\mathbf{f}_1(w,\mathbf{r},t)\cdot\frac{\mathbf{w}}{|\mathbf{w}|} \quad (3)$$

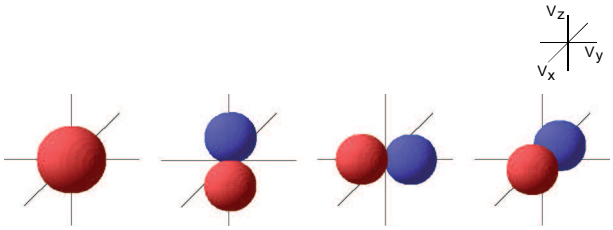

Figure 1. The angular distribution – in velocity space – of the first four cartesian tensors. From left to right: f_0, f_{1z}, f_{1y}, f_{1x}. Red represents an additive contribution to the distribution function, blue a subtractive.

We truncate the expansion after two terms – this is known as the 'diffusive' approximation. The expansion allows us to reduce the number of dimensions in the problem from five to three; the angular variation of the distribution function in velocity space is prescribed by the cartesian tensors (as shown if figure 1). The components f_0 and $\mathbf{f}_1$ are thus functions of the magnitude of the velocity only. Reducing the dimensionality of the problem allows one to solve it with a reasonable supply of computational resources. Substitution of equation (3) into equation (2) results in two coupled equations for f_0 and $\mathbf{f}_1$.

$$\underbrace{\left(\frac{\partial}{\partial t}+\mathbf{C}\cdot\nabla\right)}_{①}f_0-\underbrace{(\nabla\cdot\mathbf{C})}_{②}\frac{w}{3}\frac{\partial f_0}{\partial w}+\frac{w}{3}\nabla\cdot\mathbf{f}_1+$$
$$\frac{1}{3w^2}\frac{\partial}{\partial w}\left\{w^2\left[\mathbf{a}+\mathbf{C}\times\omega-\frac{\partial\mathbf{C}}{\partial\mathbf{t}}-(\mathbf{C}\cdot\nabla_r)\mathbf{C}\right]\cdot\mathbf{f}_1\right\}$$
$$=\underbrace{\frac{\nu'_{ee}}{w^2}\frac{\partial}{\partial w}\left[C(f_0)+D(f_0)\frac{\partial f_0}{\partial w}\right]}_{③} \quad (4)$$

$$\underbrace{\left(\frac{\partial f_{1j}}{\partial t}+C_k\frac{\partial f_{1j}}{\partial r_k}\right)}_{④}+w\frac{\partial f_0}{\partial r_j}$$
$$+\left[\omega\times\mathbf{f}_1\right]_j+\frac{\partial f_0}{\partial w}\underbrace{\left(a_j+\left[\mathbf{C}\times\omega\right]_j-\frac{\partial C_j}{\partial t}-C_k\frac{\partial C_k}{\partial r_j}\right)}_{⑤}-f_{1k}\frac{\partial C_k}{\partial r_j}$$
$$\underbrace{-\frac{w^2}{3}\left[\frac{\partial C_k}{\partial r_j}\frac{\partial}{\partial w}\left(\frac{f_{1k}}{w}\right)+\frac{\partial C_j}{\partial r_k}\frac{\partial}{\partial w}\left(\frac{f_{1k}}{w}\right)+\frac{\partial C_k}{\partial r_k}\frac{\partial}{\partial w}\left(\frac{f_{1j}}{w}\right)\right]}_{⑥}=-\nu_{ei}f_{1j} \quad (5)$$

We can see that the transformation makes the Vlasov part of the VFP equation considerably more complicated! Such an increase in difficulty is, however, preferable to a redefinition of the collision operators – Coulomb collisions of electrons with ions are naturally defined in the ion's rest-frame. In equations (5) and (6) ν_{ei} and ν_{ee} are the electron-electron and electron-ion collision frequencies respectively.

The terms marked ① – ⑥ in equations (4) and (5) are the correction terms we add to IMPACT to include the effects of ion motion. We can understand their significance by examining their form and velocity moments. Terms ① and ④ are the convective derivatives due to the motion of f_o and $\mathbf{f}_1$ at the ion velocity; term ② gives compressional heating of the isotropic part of the distribution function due to ion fluid flow. We expect such heating to only appear in the f_o equation as this controls the temperature of the plasma (through its w^2 'energy' moment). When we transform the coordinate system to one moving with the ions we are no longer in an inertial reference frame. As such we must include the effects of fictitious forces – these are represented by the terms in ③ and ⑤. The terms labeled ⑥ represent the bulk flow of momentum due to the average ion velocity.

The ions are modelled as a cold magneto-fluid. As such it is only their momentum equation which is important. When we strictly enforce quasi-neutrality and ignore displacement current effects – appropriate over timescales much longer than the plasma period – and also ignore electron inertia we derive their equation of motion.

$$\frac{\partial}{\partial t}(\rho\mathbf{C}) + \nabla_r \cdot (\rho\mathbf{C}\mathbf{C}) + \nabla_r\left(P_e + \frac{B^2}{2\mu_0}\right) = 0 \qquad (6)$$

Note that, as the ions are cold, it is electron pressure (Pe) and magnetic pressure that drive their flow.

Solution of equations (4) – (6) is now required. After writing them in finite difference form we eliminate $\mathbf{f}_1$ between equations (4) and (5)[2]. Terms ① – ⑥ are treated explicitly; the electric field and f_0 in the remaining terms are treated implicitly. Thus we form a matrix equation that we solve iteratively. Explicit numerical solution of Faraday's Law yields the magnetic field.

Simulation Results

We have used IMPACT (with no ion motion) to simulate experiments investigating non-local heat transport in a gas-jet laser-produced plasma. Several important experiments of this type have been performed at the *Janus* laser facility at Lawrence Livermore National Laboratory (LLNL). A schematic of the 'classic' example of such an experiment is shown in figure 2[4]. Recently this work has been extended by the inclusion of a large magnet around the plasma producing a magnetic field in the z-direction as indicated[5]. This has been observed to suppress the effects of non-local heat transport – as shown in figure 3. We have attempted to observe a similar effect using IMPACT.

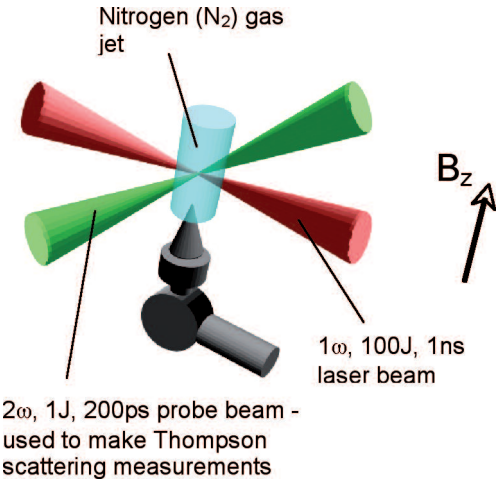

Figure 2. A schematic of experiments at LLNL using the Janus laser to investigate the effects of non-local heat transport in plasmas.

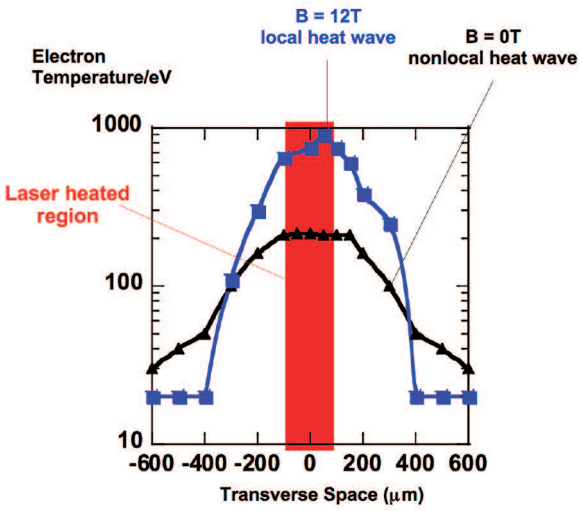

Figure 3. Temperature profiles measured after 1ns in the latest Janus experiment. The values of the externally applied B-field are given – note the pre-heated 'shoulders' in the unmagnetized plasma (figure courtesy of D.H. Froula *et al.*).

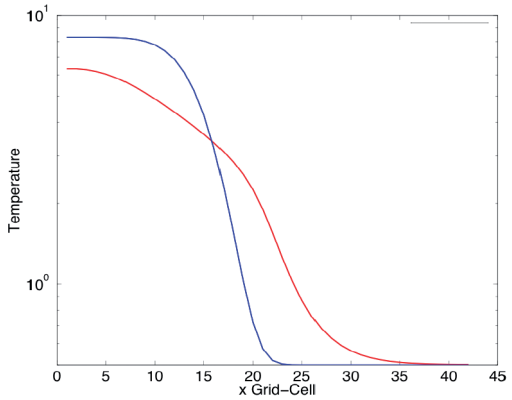

Figure 4. The temperature profiles observed in VFP simulation of non-local laser heating after 500 electron-ion collision times. The blue line has an externally applied magnetization of 133, the red line of 1.33. The laser spot is centered at (0,0).

Simulations of a circular laser spot with small and large externally applied magnetic fields were performed (magnetizations – $\omega\tau$ = 1.33 and $\omega\tau$ = 133). We give the temperature profiles of such simulations after 500 electron-ion collision times in figure 4. The interesting feature here is the 'kink' in the temperature profile for low applied magnetic field. This does not appear to be consistent with fast, relatively collisionless, electrons streaming down the temperature gradient and pre-heating the plasma (as observed experimentally). Instead it seems that the magnetic field is inhibiting heat flow in the 'kinked' region. Figure 5 shows us that the region in which the magnetic field is largest corresponds to that in which the temperature gradient is steepest (the 'kink') – supporting this idea. We see that in the highly magnetized case $\omega\tau$ = 133) the heat flow is strongly suppressed and the

'kink' disappears. Further analysis is required along with a simulation with no externally applied B-field; in such a simulation we expect to see the effects of non-local electrons pre-heating the plasma.

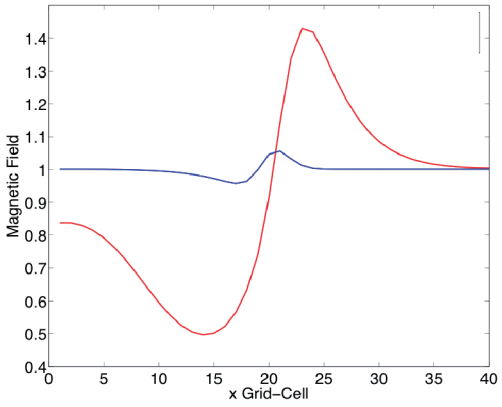

Figure 5. Magnetic field profiles after laser heating for 500 electron-ion collision times. The red line shows the simulation performed with an externally applied magnetization of 1.33, the blue line with 133. The laser spot is centered at (0,0).

We have also simulated a similar problem with ion-motion included. Here we apply a large-amplitude Gaussian temperature perturbation – with a magnitude of 0.8 times the background temperature – and watch it relax. Although the results are at a very preliminary stage, we have observed significant density modulations and qualitative differences in the magnetic field structure (compared to the case with no ion-motion). These are shown in figures 6 and 7. We see that the magnetic field is advected with the plasma; the magnetic Reynolds number is 3.8×10^4 so we expect advection of the magnetic field to dominate over its diffusion. The effect of ion-motion on the temperature profile remains to be elucidated.

We see the difference ion-motion makes to the magnetic field by comparison of figures 5 and 7. In figure 7 we see that the magnetic field has a minimum at the centre of the laser spot. This is not true of the case without ion-motion shown in figure 5. We believe that this is due to the magnetic field being moved by different processes with and without plasma motion. We postulate that the Nernst

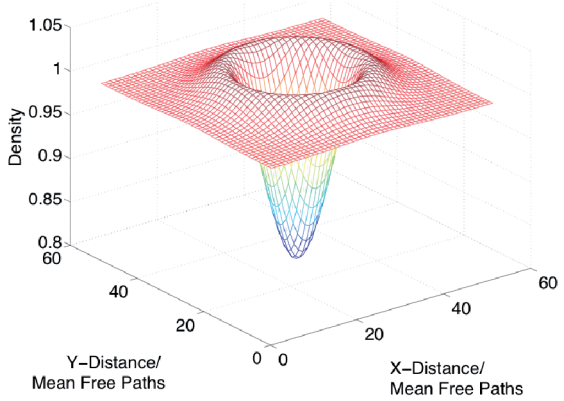

Figure 6. Density profile of the plasma after the Gaussian temperature perturbation has been allowed to relax for 100 electron-ion collision times. The laser spot is centered at (25,25) and the ions are allowed to move.

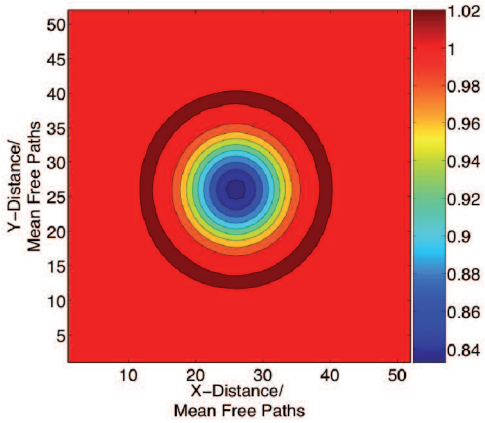

Figure 7. Magnetic field profile after the Gaussian temperature perturbation has been allowed to relax for 100 electron-ion collision times.

effect is dominant in the case where the ions are stationary whereas when the plasma moves convection of the B-field with the fluid flow is most important. This needs to be examined analytically.

Further Work

The results in figures 4 – 7 are by no means conclusive. The temperature profile in figure 4 differs qualitatively from that observed experimentally. We need to run simulations with no externally applied magnetic field for a more direct comparison. The low temperature of the background gas jet meant that – for ease of computation – we performed these preliminary simulations using rather arbitrary parameters that did not match those of the experiment. We used a higher background temperature and assumed the nitrogen was fully ionized from the outset. This should be addressed. We need to further analyse the simulations with ion-motion included – over the nanosecond timescales of interest we have shown that the bulk flow of the plasma is important. It would clearly be of interest to vary the range of magnetic fields externally applied to the plasma and observe the required value of the B-field for non-local heat flow suppression to occur with and without ion-motion.

Acknowledgements

This work was supported by the U.K EPSRC and the Rutherford Appleton Laboratory.

References

1. S. I. Braginskii, Transport Processes in a Plasma, in *Reviews of Plasma Physics, Consultants Bureau, New York*, Vol. 1, p205
2. R. J. Kingham & A. Bell, *Journal of Computational Physics,* Vol. 194, p1, 2004
3. I. P. Shkarofsky, *The Particle Kinetics of Plasmas*, Addison-Wesley, 1966
4. G. Gregori *et al.*, *Physical Review Letters,* Vol. 92, No. 20, p205006-1, 2004
5. D. H. Froula *et al.*, *Private Communication*